A New Simple Analytical Method for a Highly Accurate Determination of the Optical Parameters of a Slab from Transmittance Data

van Huy Mai, Alexandre Jaffré, Khai Doan, Duc Thien Trinh, Olivier Schneegans

A new simple analytical method for a highly accurate determination of the optical parameters of a slab from transmittance data

Van Huy Mai[1], Alexandre Jaffré[2], Khai Minh Doan[1], Duc Thien Trinh[3], Olivier Schneegans[2]

1 Le Quy Don Technical University, Hanoi, Vietnam
2 Laboratoire Génie Électrique et Électronique de Paris, CentraleSupélec, UMR8507 CNRS, Université Paris-Saclay, Sorbonne Université, Gif-sur-Yvette, France
3 Faculty of Physics, Hanoi National University of Education, Hanoi, Vietnam

Corresponding author:
Olivier Schneegans, GeePs Laboratory, 11 rue Joliot-Curie, 91192 Gif-Sur-Yvette, France
Email: olivier.schneegans@geeps.centralesupelec.fr

Abstract

To date, determining with high accuracy the optical parameters (extinction coefficient *k* and refractive index *n*) of a slab from the sole transmittance data requires an inverse method based on numerical iteration procedures. In this paper, we propose a new inverse analytical method of extracting (*k*, *n*) without numerical iterative processes. The high accuracy of this new inverse method is assessed, and as an application example, the optical parameters of CaF_2 and Si substrates are determined in the IR spectral range of 4-8 µm.

Keywords: optical constants, extinction coefficient, refractive index, transmittance, analytical modeling, calcium fluoride, silicon.

Introduction

The optical properties of a material depend on two main parameters: the refractive index *n*, which is related to the wave propagation velocity inside the material, and the extinction coefficient *k*, which is linked to the wave intensity attenuation due to absorption by the constitutive molecules of the material. Accurate knowledge of *k* and *n* over a wavelength range is of crucial importance for many optical applications, from laser windows and fiber optic systems[1,2] (for which low-absorption materials are used) to thin-film optical coatings, whose characteristics depend on the refractive indices of the substrates and the thin films deposited.[3-5]

Since *k* and *n* cannot be simultaneously determined directly, a usual strategy consists of measuring two other parameters and then employing an inverse procedure to obtain *k* and *n*. Typical methods include the following spectrophotometry measurements:

- the use of Kramers-Kronig analysis of transmittance *T*, which enables the calculation of a phase shift (φ): the knowledge of *T* and φ allows then the extraction of (*k*, *n*).[6,7] However, this requires a numerical iteration inversion and the measurement of *T* over a maximum possible wavelength range,
- reflectance *R* and transmittance *T* of a single slab:[8] numerical iteration procedures have first been proposed to solve the (*R*, *T*)→(*k*, *n*) inverse problem.[9-11] Later, exact analytical solutions have been found and applied to the study of slabs.[12-15] The main challenge lies here in the fact that measuring *R* and *T* at the same location is difficult.[6] Moreover, materials with low refractive index yield weak reflection, thus the precise measurement of *R* appears tricky in this case,[16,17]
- transmittance of several samples of the same material: this (T_1, T_2)→(*k*, *n*) method has been applied to one-layer structures (solid slabs[18-20] or liquids in a simplified model[17]), as well as to three-layer structures to determine the optical parameters of liquids.[21-24] In all the cases, the (T_1, T_2)→(*k*, *n*) inverse problem corresponds to a set of nonlinear equations, which are too complex to be solved mathematically; hence, numerical iterative techniques have been used. These methods are inherently confronted with difficulties, such as convergence towards several possible values[16,22] or slow convergence speed.[18,19] To overcome such difficulties, different strategies have been proposed recently, such as faster iterative algorithms[20,22] or a combined transmittance-ellipsometry approach[16,23,24] which also includes a numerical iterative step.

In the one-layer structure, using highly accurate analytical expressions to solve the (T_1, T_2)→(*k*, *n*) inverse problem would represent an obvious advantage over numerical iteration processes. However, to date, there is no analytical inverse method, which allows *k* to be obtained with high accuracy, similar to what iterative calculations can achieve. The only well-known classical analytical inverse method (CAIM) allows the derivation of the absorption coefficient α (hence the extinction coefficient *k*), using[9]

$$\alpha = \frac{1}{(d_2 - d_1)} . \ln\left(\frac{T_1}{T_2}\right) \Rightarrow k = \frac{\lambda}{4\pi.(d_2 - d_1)} . \ln\left(\frac{T_1}{T_2}\right) \quad (1)$$

where T_1 (resp. T_2) is the transmittance for the sample with thickness d_1 (resp. d_2) at wavelength λ.

However, Eq. (1) is only considered as a rough estimation,[9] and for high-refractive-index materials, it may at first sight result in relative errors on *k* and *n* reaching up to 45% or more.[25]

In this study, after precisely specifying the accuracy of the CAIM, we proposed a novel method to obtain the extinction coefficient *k* and the refractive index *n* of a slab from T_1 and T_2 measurements at normal incidence (Figure 1) by establishing analytical expressions, that yield highly accurate (*k*, *n*) values.

The accuracy of our new analytical inverse method (NAIM) was studied and assessed. As an application example, we then determined the optical parameters of CaF_2 (low-refractive-index material) and Si (high-refractive-index material) and compared their values with literature data.

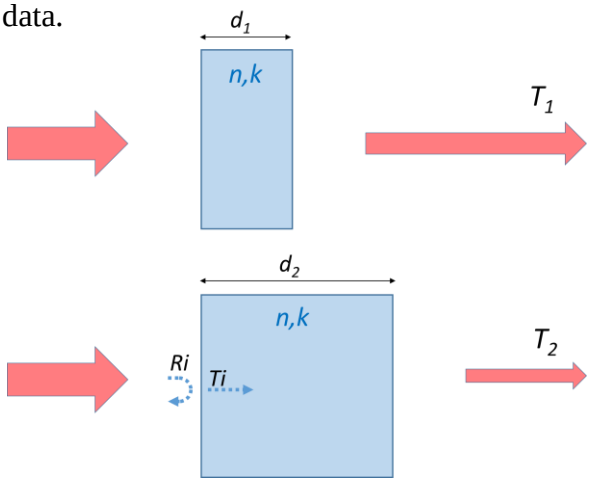

Figure 1. Schematic view of two samples of thicknesses d_1 and d_2 ($d_2 > d_1$) of the same material, yielding transmittance T_1 and T_2 ($T_2 < T_1$). The coefficients *Ri*, *Ti* are the Fresnel intensity reflectance and transmittance coefficients of a single slab face at normal incidence. These Fresnel intensity coefficients (only drawn on the thickest sample for clarity) do not depend on the thickness of the slab.

Determination of the accuracy of the classical analytical inverse method (CAIM)

Test procedure to establish the accuracy of an inverse method

To obtain the accuracy of a (T_1, T_2)→(k, n) inverse method, two different thicknesses (d_1 and d_2) were used as references. The two thicknesses should not be too close to each other so that the transmittance curves may appear better separated. Besides, optical windows with thicknesses below 10mm are easy to carry out experiments with (and are easily commercially available). Therefore d_1 = 2mm and d_2 = 8mm were selected as the thickness references for the analysis.

Next, we describe a test procedure (summarized in Figure 2) that will be applied in the subsequent sections. First (step 1), for a given wavelength λ, assigning k values in the range [10^{-7}-10^{-3}] and n values in the range [1.4 - 4.0] allows the calculation of the intensity reflectance coefficient *Ri* (using the Fresnel equations) and the attenuation coefficient α expressed as follows:

$$Ri = \frac{(n-1)^2+k^2}{(n+1)^2+k^2} \quad \text{and} \quad \alpha = \frac{4\pi.k}{\lambda} \tag{2}$$

The transmission T of the slab (of thickness d) is then given by the exact analytical expression below, which takes into account the multiple reflection contributions at the front and back air/sample interfaces:[8,12]

$$T = \frac{(1-Ri)^2.e^{-\alpha.d}}{1-Ri^2.e^{-2.\alpha.d}} \tag{3}$$

Hence (step 2) transmittances T_1 and T_2 can be computed with arbitrary precision using Eq. (3), which corresponds to the direct problem. Once T_1 and T_2 are known, trying to solve the (T_1, T_2)→(k, n) inverse problem leads to the following set of two nonlinear equations, where *Ri* and α are the two unknowns:

$$\begin{cases} T_1 = \frac{(1-Ri)^2.e^{-\alpha.d_1}}{1-Ri^2.e^{-2.\alpha.d_1}} \\ T_2 = \frac{(1-Ri)^2.e^{-\alpha.d_2}}{1-Ri^2.e^{-2.\alpha.d_2}} \end{cases} \tag{4}$$

This set of equations (Eq. (4)) appears too complex to be solved analytically; thus, approximate values of *Ri* and α have to be computed, which then yield (by solving Eq. (2)) approximate values k_{ap} and n_{ap} (step 3). Finally, (step 4) k_{ap} may be compared to k (through percent error *PEk*), and n_{ap} may be compared to n (through absolute error Δn), as follows:

$$PEk = 100.\left|\frac{k_{ap}-k}{k}\right| \qquad \Delta n = \left|n_{ap} - n\right| \tag{5}$$

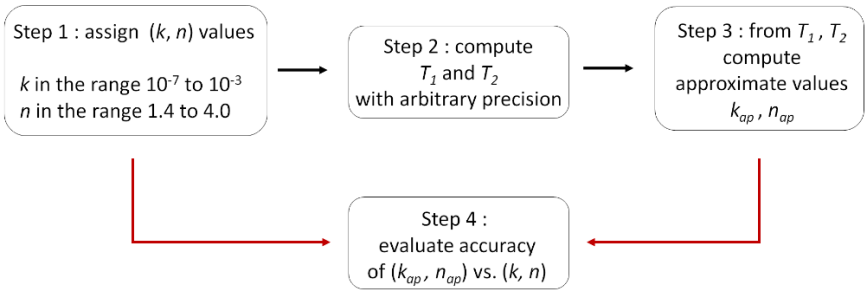

Figure 2. Schematic view of the steps to study the accuracy of approximate values (k_{ap}, n_{ap}) of (k, n)

Application: determination of the accuracy of the classical analytical inverse method

Starting from the following analytical expression of the transmittance:[8]

$$T = \frac{(1-Ri)^2.e^{-\frac{4\pi.k.d}{\lambda}}}{1-Ri^2.e^{-\frac{8\pi.k.d}{\lambda}}} \tag{6}$$

the denominator may be approximated by 1 if $Ri \ll 1$ (this is the case for low-refractive index materials such as glasses), or if $e^{-\frac{8\pi.k.d}{\lambda}} \ll 1$ (which happens if the material is highly absorbent at the considered wavelength and thickness). Under these assumptions, Eq. (6) may be simplified as:

$$T = (1 - Ri)^2.e^{-\frac{4\pi.k.d}{\lambda}} \tag{7}$$

Thus, the k parameter is easy to obtain and corresponds to the classical analytical inverse method (CAIM):[9]

$$k = \frac{\lambda}{4\pi.(d_2-d_1)}.\ln\left(\frac{T_1}{T_2}\right) \tag{8}$$

Once k is known, *Ri* can be computed using Eqs. (6) or (7), using the T_1 data for the less thick sample (d_1). Note that deducing *Ri* in terms of k and T using Eq. (6) yields a much more accurate *Ri* value than that obtained using Eq. (7). Hence only Eq. (6) is considered here: this 2nd order equation can be solved analytically, yielding the only acceptable solution for *Ri* (satisfying $Ri < 1$):

$$Ri = \frac{1-T_1.\sqrt{1+\frac{1}{T_1.Y_1}-\frac{Y_1}{T_1}}}{1+T_1.Y_1} \quad \text{with} \quad Y_1 = e^{-\frac{4\pi.k.d_1}{\lambda}} \tag{9}$$

From *Ri*, the refractive index n can be obtained by solving Eq. (2), yielding the following formula:

$$n = \frac{1+Ri}{1-Ri} + \sqrt{\frac{4.Ri}{(1-Ri)^2} - k^2} \approx \frac{1+\sqrt{Ri}}{1-\sqrt{Ri}} \tag{10}$$

Figure 3 shows the accuracy of the CAIM for determining k and n.

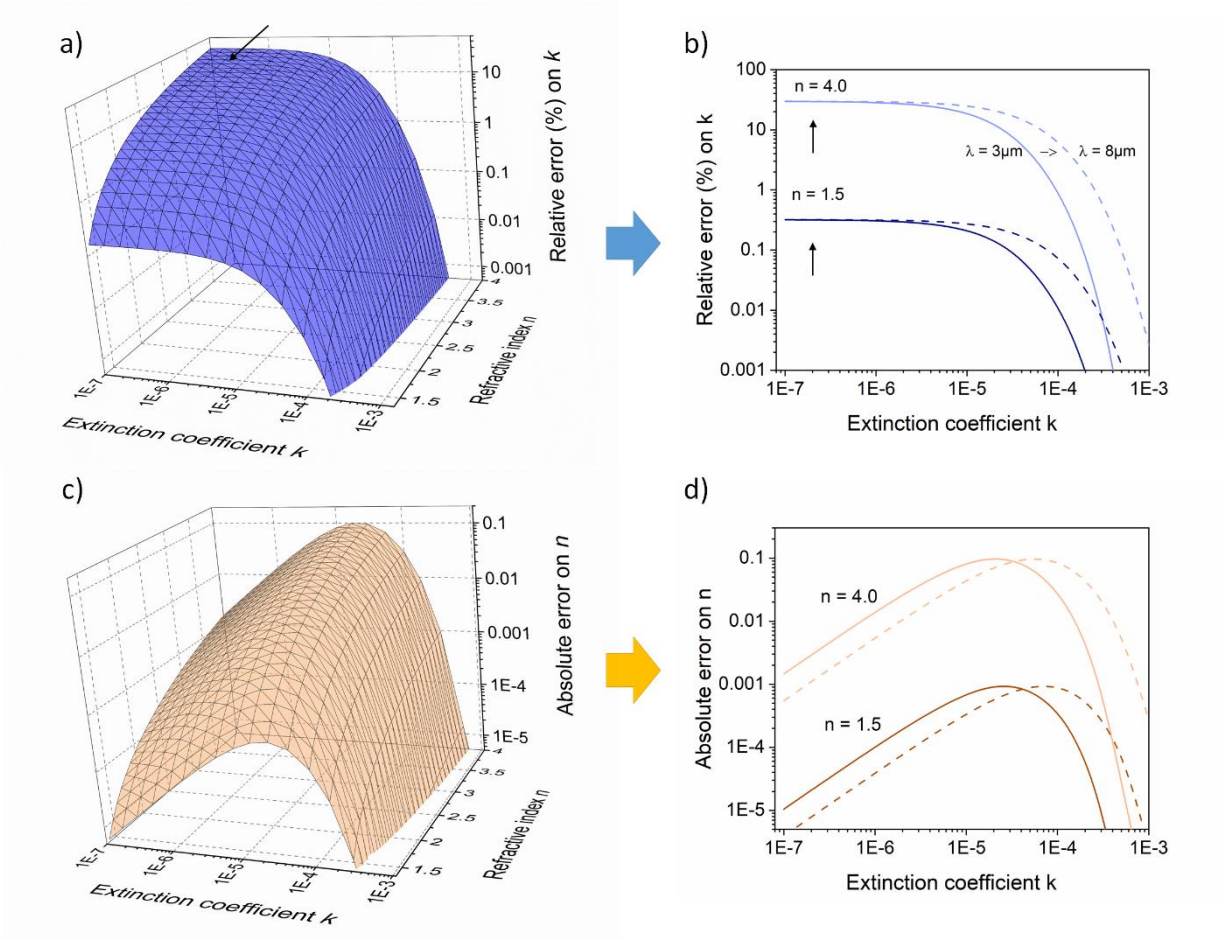

Figure 3. Using the classical method (CAIM) leads to the following quantified errors (a) *PEk* percent error on the determination of *k* (b) *PEk* percent error on *k*, for two values of *n* (1.5 and 4), for λ = 3μm (solid curves) and for λ = 8μm (dashed curves) (c) Δ*n* absolute error on the determination of *n* (d) Δ*n* absolute error on *n* for two values of *n*, for λ = 3μm (solid curves) and for λ = 8μm (dashed curves)

Concerning the accuracy of the CAIM in determining the coefficient *k*, it can first be noted that the highest percent error values, reaching ~ 30% (Figure 3a, black arrow), occur for high refractive indices and low extinction coefficients. Moreover, for a given refractive index *n* (Figure 3b), all the *PEk* percent error curves appear constant for low *k* values, then decrease for increasing values of *k*. Hence the maximum of a *PEk* curve, denoted max(*PEk*), is defined, and depends on the *n* value (fig 3b); it can be seen that max(*PEk*) increases with *n*: max(*PEk*) ≈ 0.3% for *n* = 1.5, and max(*PEk*) ≈ 30% for *n* = 4. In addition, changing the considered wavelength λ only shifts the *PEk* curves horizontally (Figure 3b, λ = 3 μm and λ = 8 μm): the curve maximum stays at the same value (black arrows); hence, max(*PEk*) does not depend on λ and can be defined as the global maximum percent error on *k* of the CAIM for a given *n*. In concrete cases, *n* and *k* depend on λ, hence the *k*(λ) and *n*(λ) curves can be viewed as particular (*k*, *n*) sets whose maximum percent error on *k* is most often lower than (or in the worst case, equal to) max(*PEk*), using the highest *n* value of *n*(λ).

Concerning the accuracy of the CAIM in deriving the refractive index *n* (Figure 3c,d), it can be observed that for a given value of *n*, all the Δ*n* curves (Figure 3d) go through a maximum, which is higher for high refractive indices *n*. Hence the Δ*n* curve maximum, denoted max(Δ*n*), is defined and depends on the *n* value. For *n* = 1.5, max(Δ*n*) ≈ 0.001,

which corresponds to an accuracy of one unit on the 3rd decimal place. However, for n = 4, max(Δn) reaches ≈ 0.1 (error of one unit on the 1rst decimal place). This underlines that the CAIM appears unsuitable for high-refractive-index materials. A change in λ also shifts the Δn curves only horizontally (Figure 3d, λ = 3 µm for the solid curve and λ = 8 µm for the dashed curve); hence, max(Δn) does not depend on λ or k, and can be defined as the global maximum absolute error on n of the CAIM for a given n.

Hereafter, a new analytical expression for k is established, whose much higher accuracy allows (through Eqs. (9-10)) derivation of n with a much higher accuracy.

New analytical expression for the extinction coefficient *k*

Mathematical modeling

Starting from the following analytical expression of the transmission T:

$$T = \frac{(1-Ri)^2.e^{-\alpha.d}}{1-Ri^2.e^{-2.\alpha.d}} \tag{11}$$

And taking the logarithm of both sides leads to:

$$\ln(T) = \ln((1-Ri)^2) - \alpha.d - \ln(1-Ri^2.e^{-2.\alpha.d}) \tag{12}$$

The last term can be rewritten, by using, for x such that $0<x<1$, the approximation:

$$-\ln(1-x) \approx x \quad \Rightarrow \quad -\ln(1-Ri^2.e^{-2.\alpha.d}) \approx Ri^2.e^{-2.\alpha.d} \tag{13}$$

A simpler expression is thus obtained:

$$\ln(T) \approx \ln((1-Ri)^2) - \alpha.d + Ri^2.e^{-2.\alpha.d} \tag{14}$$

In Eq. (14), the last term appears complex to handle. First, $e^{-2.\alpha.d}$ may be expressed in terms of T. For this, we use Eq. (11) again, assuming that in Eq. (11) $e^{-2.\alpha.d} \approx 1$ (valid in the transparent region). This yields:

$$T \approx \frac{(1-Ri)^2}{1-Ri^2}.e^{-\alpha.d} = \frac{1-Ri}{1+Ri}.e^{-\alpha.d} \tag{15}$$

Therefore, we have

$$e^{-2.\alpha.d} \approx \left(\frac{1+Ri}{1-Ri}\right)^2.T^2 \tag{16}$$

Replacing then Eq. (16) in Eq. (14) leads to:

$$\ln(T) \approx \ln((1-Ri)^2) - \alpha.d + Ri^2.\left(\frac{1+Ri}{1-Ri}\right)^2.T^2 \tag{17}$$

The set of equations for the two thicknesses d_1 and d_2 can thus be written as follows:

$$\begin{cases} \ln(T_1) \approx \ln((1-Ri)^2) - \alpha.d_1 + Ri^2.\left(\frac{1+Ri}{1-Ri}\right)^2.{T_1}^2 \\ \ln(T_2) \approx \ln((1-Ri)^2) - \alpha.d_2 + Ri^2.\left(\frac{1+Ri}{1-Ri}\right)^2.{T_2}^2 \end{cases} \tag{18}$$

The coefficient α (and consequently k) can be retrieved by subtracting the two preceding expressions:

$$k = \frac{\lambda}{4\pi}.\alpha = \frac{\lambda}{4\pi.(d_2-d_1)}.\left[\ln(T_1/T_2) - \left(Ri^2.\left(\frac{1+Ri}{1-Ri}\right)^2\right).\left({T_1}^2 - {T_2}^2\right)\right] \tag{19}$$

It then remains to find an expression for *Ri*, which may be precise enough to be used in Eq. (19). For this, assuming $e^{-2.\alpha.d} \approx 1$ (valid in the transparent region), Eq. (12) can be simplified:

$$\ln(T) = \ln((1-Ri)^2) - \alpha.d - \ln(1-Ri^2) \tag{20}$$

which leads to :

$$\ln(T) = \ln\left(\frac{1-Ri}{1+Ri}\right) - \alpha.d \tag{21}$$

Then using T_1 and T_2, the following set of equations is obtained:

$$\begin{cases} \ln(T_1) = \ln\left(\frac{1-Ri}{1+Ri}\right) - \alpha.d_1 \\ \ln(T_2) = \ln\left(\frac{1-Ri}{1+Ri}\right) - \alpha.d_2 \end{cases} \tag{22}$$

Eliminating α from the two equations, we have:

$$\ln\left(\frac{1-Ri}{1+Ri}\right) = \frac{d_2.\ln(T_1) - d_1.\ln(T_2)}{d_2 - d_1} \tag{23}$$

Thus, *Ri* can be expressed as follows:

$$Ri = \frac{1-e^{-C}}{1+e^{-C}} = \tanh(C/2) \quad \text{with} \quad C = \frac{d_1.\ln(T_2) - d_2.\ln(T_1)}{d_2 - d_1} > 0 \tag{24}$$

Therefore the final simple expression of *k* as a function of T_1, T_2, d_1, d_2 is:

$$k = \frac{\lambda}{4\pi.(d_2 - d_1)}.\left[\ln(T_1/T_2) - N.\left({T_1}^2 - {T_2}^2\right)\right] \tag{25}$$

with

$$N = \left(e^C.tanh(C/2)\right)^2 \quad \text{and} \quad C = \frac{d_1.\ln(T_2) - d_2.\ln(T_1)}{d_2 - d_1}$$

To get *n*, Eqs. (9) and (10) are used.

Accuracy of the new analytical inverse method (NAIM)

Figure 4 shows the comparative accuracies of the NAIM and the CAIM for λ = 3µm. The accuracies of both methods are shown for a low refractive index (*n* = 1.5, Figure 4a,b), which is interesting because many types of glasses have refractive indices close to this value. For *k*, the new method leads to a maximum percent error of 0.001% (Figure 4a), which is more than two orders of magnitude better than the classical method (≈ 0.3%). For *n*, Figure 4b shows that the new method yields an accuracy of ±0.00001, which is two decades better than the classical method (max(Δ*n*) ≈ 0.001).

The accuracies of the NAIM and the CAIM are also shown for silicon, which is a high-refractive-index material (*n* = 3.4, Figure 4c,d). For *k*, the new method (Figure 4c) results in a maximum percent error of ≈1.5% (compared to ≈ 20% with the classic method). For *n* (Figure 4d), the accuracy reaches ±0.004, which is 25 times better than that of the classical method (±0.1).

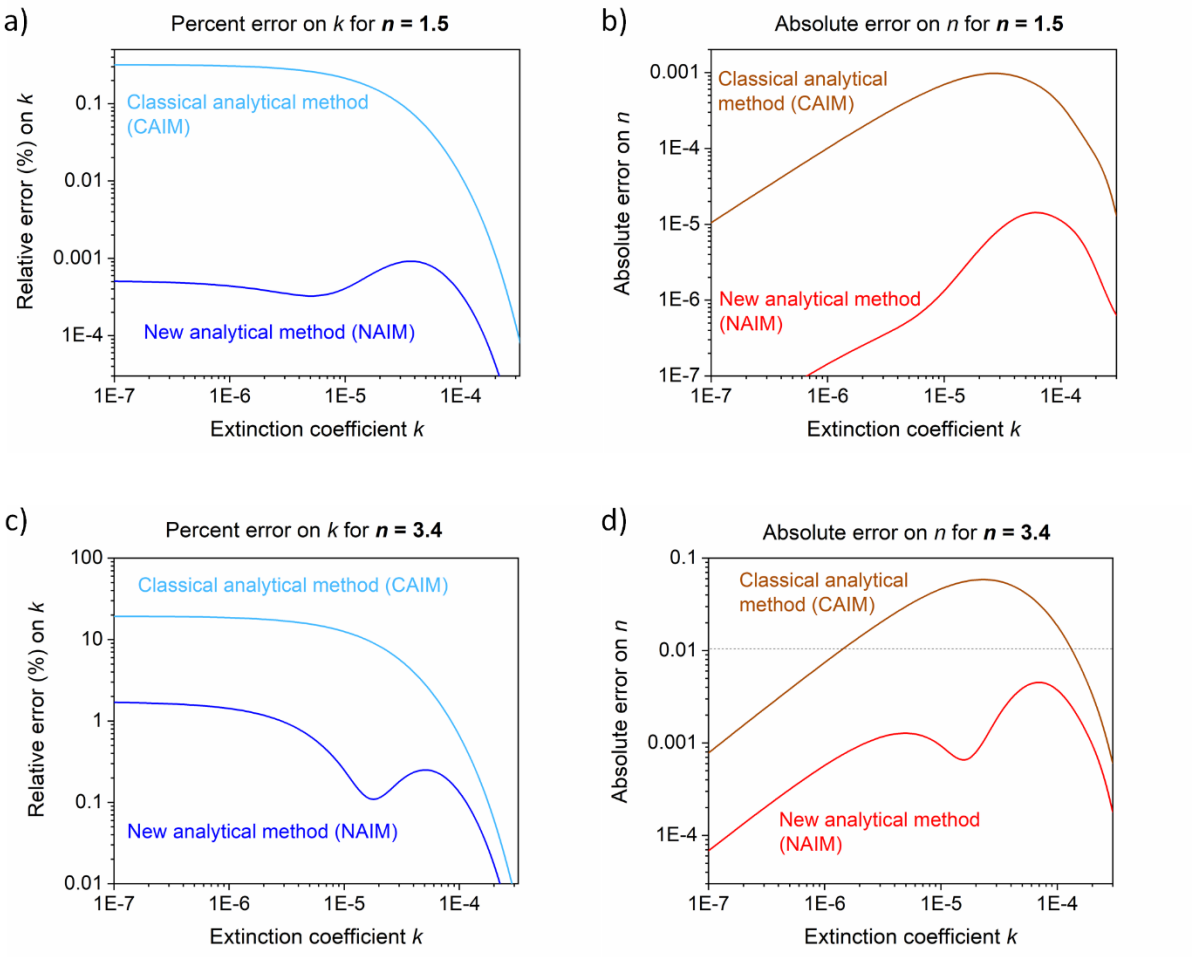

Figure 4. Comparative accuracies of the CAIM and the NAIM in the determination of (*k*,*n*); (a) *PEk* for *n* = 1.5 (b) Δ*n* for *n* = 1.5 (c) *PEk* for *n* = 3.4, and (d) Δ*n* for *n* = 3.4; the dotted line represents an absolute error of 1 digit on the second decimal place of *n*.

Application example: determination of (*k*, *n*) for CaF_2 and Si

The transmittance of CaF_2 and Si optical samples (circular slabs) was measured at normal incidence in the 4-8μm IR range, using a Spectrum 400 FT-IR spectrometer (Perkin Elmer Company) with a MCT detector; the resolution was set to 4 cm^{-1} (the transmittance curves are shown in the Supplemental Material S1, and the raw data are available as supplemental files). The possible sources of transmittance uncertainties are multiple (e.g. detector nonlinearity, defocusing effects, etc…).[26,27] In our case, the accuracy of the FTIR instrument was estimated at ±0.1% (similar to literature data[28]). Moreover, in opaque regions, we observed that the transmittance noise level and the systematic errors were lower than 0.1%. Hence $\sigma_T = 0.2\%$ was taken as an estimate of the standard deviation of the measured transmittance.

Figure 5a,b shows the determined (*k*, *n*) parameters of CaF_2 optical windows (thickness d_1 = 2.00mm and d_2 = 8.00mm, supplier: Crystran Company, UK). In the 4-8μm range, *k* increases with wavelength from 3×10^{-7} to 1×10^{-5}. These values are quantitatively in very good agreement with recently published data.[29] The *n* values (Figure 5b), which decrease with the wavelength from about 1.41 to 1.36, are also in very good agreement with literature data.[29,30] The standard deviation of transmittance chosen (σ_T = 0.2%) yields uncertainties of ±0.01 for *n*. For *k*, the error results in the highly transparent region ($k < 10^{-6}$) may be further lowered using thicker samples.

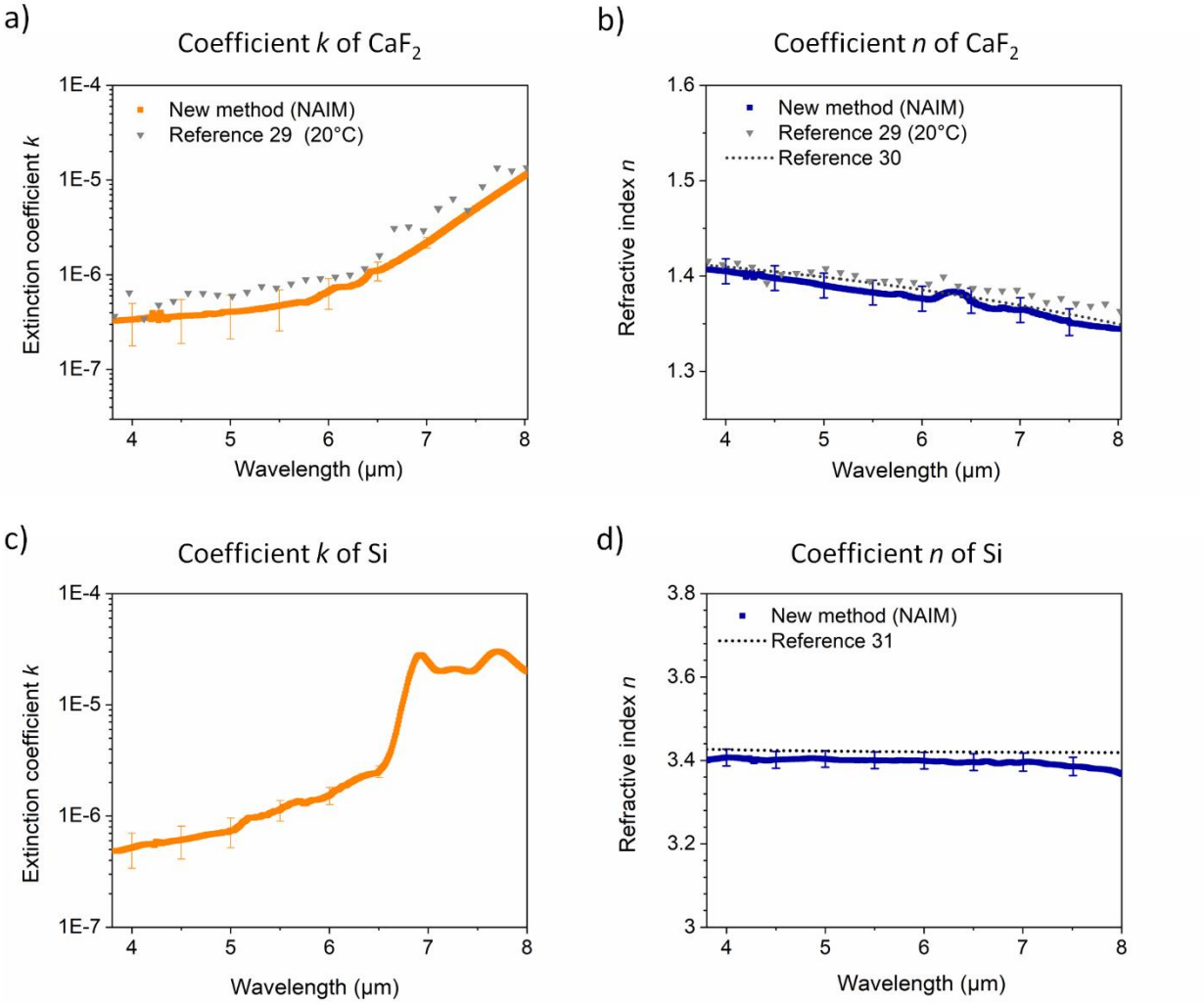

Figure 5. Determination of (*k*, *n*) of CaF_2 and FZ-Si windows using the NAIM (a) Extinction coefficient *k* of CaF_2 (NAIM), and *k* data from Reference 29 (b) Refractive index *n* of CaF_2 (NAIM), and *n* data from References 29 and 30 (c) Extinction coefficient *k* of FZ-Si (NAIM) (d) Refractive index *n* of FZ-Si (NAIM), and *n* data from Reference 31.

Figure 5c,d shows the determined (*k*, *n*) parameters of FZ-Si optical windows (thickness d_1 = 2.06mm and d_2 = 10.01mm, supplier : ATS Company, China). The thickness d_2 considered here is a little higher than 8mm, but it has been verified that the results shown in Fig. 4c,d remain valid. In the 4-8µm range, using the NAIM leads to an extinction coefficient *k* (Figure 5c) which increases with the wavelength from 5×10^{-7} to $\sim3\times10^{-5}$, with an abrupt change around λ = 6.5µm. For *n* (Figure 5d), using the NAIM results in a refractive index *n* which decreases slightly from 3.41 to 3.38, which is in good agreement with literature data.[31]

The small difference with the published data (≤0.02 absolute difference with reference 31 at 5µm) may be attributed to the different quality of our FZ-Si samples, or to the accuracy limit of the transmittance measurements:[26-28] indeed, the chosen standard deviation of transmittance (σ_T = 0.2%) yields uncertainties of ±0.02 for *n*.

It can be noted that the errors arising from the new analytical calculation of *n* from transmittances T_1 and T_2 are negligible (≤ 0.00001 for CaF_2 and ≤ 0.004 for Si), compared to the errors in *n* (±0.01 for CaF_2 and ±0.02 for Si) owing to the experimental measurement

uncertainties on T_1 and T_2. Thus two limitations of the present method may be considered: for highly transparent samples, T_1 and T_2 may be too close to each other to be well-separated (hence thicker samples may be used, in a reasonable range to explore). Conversely, for regions with very high absorption, the transmittance is too low to be measured by FTIR; in this case, our method cannot be used, and alternative methods (e.g., reflectance spectroscopy,[32,33] ellipsometry[16]) are effective for measuring high k values (> 10^{-3}).

Conclusions

In this study, we proposed a new analytical inverse method (NAIM) to extract the optical constants (k, n) of a solid material with high accuracy from transmittance data of samples with two different thicknesses (in the range 2-10mm), without any numerical iterative process. To this end, we established easy-to-use analytical expressions for k and n. Given transmittance data, the NAIM is used to solve the (T_1, T_2)→(k, n) inverse problem with high accuracy (e.g. 0.00001 for n in the case n = 1.5, and 0.004 for n in the case n = 3.4). As an illustrative example, the (k, n) optical parameters of two materials (CaF_2 and FZ-Si) were determined straightforwardly in the 4-8µm IR spectral range, and the results obtained are in very good agreement with published data. Hence this new method may be a useful alternative for deriving the optical constants of solid materials with high accuracy.

Acknowledgments

This work was supported by the French National Research Agency (ANR-19-CE09-0013) and by the Le Quy Don Technical University (under grant number 20.1.028).

Conflict of interest

The authors report there are no conflicts of interest

References

1. H. Piombini, A. Guediche, D. Picart, G. Dammame. “Absorption measurements of layers or materials: how to calibrate ?”. Results in Physics. 2019. 14: 102314

2. D.C. Tran, G.H. Sigel Jr, B. Bendow. “Heavy Metal Fluoride Glasses and Fibers: A review”. J. of Lightwave Technology. 1984. 2(5): 566-586

3. U. Schulz et al. “Part IV : Applications of optical thin films and coatings”. In: A. Piegari, F. Flory, editors. Optical Thin Films and Coatings: from Materials to Applications (2nd edition). Duxford, UK: Woodhead Publishing, 2018. Chap. 13-22. Pp. 517-810

4. O. Stenzel. “Thin Films, Substrates, and Multilayers”. In: G. Ertl, H. Lüth, D.L. Mills, editors. Optical Coatings – Material Aspects in Theory and Practice. Berlin

Heidelberg, Germany: Springer Verlag, 2014. Vol. 54. Chap. 4. Pp. 81-113

5. J.A. Dobrowolski. “Optical properties of films and coatings”. In: M. Bass, editor. Handbook of Optics Volume I: Fundamentals, Techniques, and Design (2nd edition). New York, USA: McGraw-Hill, 1995. Chap. 42. Pp. 42.1 - 42.128

6. D. Poelman, P.F. Smet. “Methods for the determination of the optical constants of thin films from single transmission measurements: a critical review”. J. Phys. D: Appl. Phys. 2003. 36: 1850-1857

7. K.F. Palmer, M.Z. Williams, B.A. Budde, “Multiply subtractive Kramers–Kronig analysis of optical data”. Applied Optics. 1998. 37(13): 2660-2673

8. O. Stenzel. “Thick Slabs and Thin Films”. In: R. Car, G. Ertl, H.J. Freund, H. Lüth, M.A. Rocca, editors. The Physics of Thin Film Optical Spectra – An introduction (Second Edition). Berlin Heidelberg, Germany: Springer, 2016. Vol. 44. Chap. 7. Pp. 131-138

9. O. Stenzel, V. Hopfe, P. Klobes. “Determination of optical parameters for amorphous thin film materials on semi-transparent substrates from transmittance and reflectance measurements”. J. Phys. D: Appl. Phys. 1991. 24: 2088-2094

10. M.A. Khashan, A.M. El-Naggar. “A new method of finding the optical constants from the reflectance and transmittance spectrograms of its slab”. Optics Communications. 2000. 174: 445-453

11. M.A. Khashan, A.Y. Nassif. “Determination of the optical constants of quartz and polymethyl-methacrylate glasses in a wide spectral range: 0.2-3μm”, Optics Communications. 2001. 188: 129-139

12. E. Nichelatti. “Complex refractive index of a slab from reflectance and transmittance: analytical solution”. J. Opt. A: Pure Appl. Opt. 2002. 4: 400-403

13. S.Y. El-Zaiat, M.B. El-Den, S.U. El-Kameesy, Y.A. El-Gammam. “Spectral dispersion of linear optical properties for Sm_2O_3 doped B_2O_3–PbO–Al_2O_3 glasses”. Optics and Laser Technology. 2012. 44: 1270-1276

14. S.Y. El-Zaiat. “Determination of the complex refractive index of a thick slab material from its spectral reflectance and transmittance at normal incidence”. Optik. 2013. 124: 157-161

15. E.-S.Y. El-Zaiat, G.M. Youssef. “Dispersive parameters for complex refractive index of p- and n-type silicon from spectrophotometric measurements in spectral range 200–2500 nm”. Optics & Laser technology. 2015. 65: 106-112

16. X. Li, C. Wang, J. Zhao, L. Liu. “A New Method for Determining the Optical Constants of Highly Transparent Solids”. Appl. Spectrosc. 2017. 71(1): 70-77

17. A. Tuntomo, C.L. Tien, S.H. Park. “Optical constants of liquid hydrocarbon fuels”,

Combust. Sci. and Technol. 1992. 84: 133–140

18. D. Li, Q. Ai, X. Xia. “Measured optical constants of ZnSe glass from 0.83 μm to 2.20μm by a novel transmittance method”. Optik. 2013. 124: 5177-5180

19. H. Qi, X. Zhang, M. Jiang, C. Liu, Q. Wang, D. Li. “Optical properties of zinc selenide slabs at 373 and 423 K in the wavelength 2–15 μm”. Optik. 2016. 127: 5576-5584

20. X. Hu, T. Xu, L. Zhou, Q. Wang, M. Arici, D. Li. “Comparison of transmittance and reflection methods for solving optical constants of optical glass”. Optik. 2019. 183: 924-932

21. X. Li, L. Liu, J. Zhao, J. Tan. “Optical Properties of Sodium Chloride Solution Within the Spectral Range from 300 to 2500 nm at Room Temperature”. Appl. Spectrosc. 2015. 69(5): 635-640

22. Q. Ai, M. Liu, C. Sun, X. Xia. “Temperature Dependence of Optical Constants for Chinese Liquid Hydrocarbon Fuels in the Near-Infrared (NIR) Region from Room Temperature to 400 K”. Appl. Spectrosc. 2017. 71(8): 2026-2033

23. C.C. Wang, J.Y. Tan, Y.Q. Ma, L.H. Liu. “Infrared optical constants of liquid palm oil and palm oil biodiesel determined by the combined ellipsometry-transmission method”. Applied Optics. 2017. 56(18): 5156-5163

24. X. Li, B. Xie, M. Wu, J. Zhao, Z. Xu, L. Liu. “Visible-to-near-infrared optical properties of protein, lipid and carbohydrate in both solid and solution state at room temperature”. Journal of Quantitative Spectroscopy & Radiative Transfer. 2021. 259: 107410

25. E.N. Kotlikov. “A spectrophotometric method for determination of the optical constants of materials”. J. Opt. Technol. 2016. 83(2): 77-80

26. S.G. Kaplan, L.M. Hanssen, R.U. Datla, “Testing the radiometric accuracy of Fourier transform infrared transmittance measurements”. Applied Optics. 1997. 36(34): 8896-8908

27. T.F. Deutsch. “Absorption coefficient of infrared laser window materials”. J. Phys. Chem. Solids. 1973. 34: 2091-2104

28. B.T. Bowie, P.R. Griffiths. “Measurement of the Sensitivity and Photometric Accuracy of FT-IR Spectrometers”. Appl. Spectrosc. 2000. 54(8): 1192-1202

29. X.C. Li, C.C. Wang, J.M. Zhao, L.H. Liu. “Temperature-dependent optical constants of highly transparent solids determined by the combined double optical pathlength transmission-ellipsometry method”. Applied Optics. 2018. 57(5): 1260-1266

30. I.H. Malitson. “A Redetermination of Some Optical Properties of Calcium

Fluoride". Applied Optics. 1963. 2(11): 1103-1107

31. D. Chandler-Horowitz, P.M. Amirtharaj. "High-accuracy, midinfrared (450 $cm^{-1} \leq \varpi \leq 4000\ cm^{-1}$) refractive index values of silicon". J. Appl. Phys. 2005. 97: 123526

32. M.R.K. Kelly-Gorham, B.M. DeVetter, C.S. Brauer, B.D. Cannon, S.D. Burton, M. Bliss, T.J. Johnson, T.L. Myers. "Complex refractive index measurements for BaF_2 and CaF_2 via single-angle infrared reflectance spectroscopy". Optical Materials. 2017. 72: 743-748

33. T.P. de Silans, I. Maurin, P.C.d.S. Segundo, S. Saltiel, M.-P. Gorza, M. Ducloy, D. Bloch, D.d.S. Meneses, P. Echegut. "Temperature dependence of the dielectric permittivity of CaF_2, BaF_2 and Al_2O_3: application to the prediction of a temperature-dependent van der Waals surface interaction exerted onto a neighbouring $Cs(8P_{3/2})$ atom". J. Phys. Condens. Matter. 2009. 21: 255902